

Theoretical Modelling and Mechanistic Study of the Formation and Atmospheric Transformations of Polycyclic Aromatic Compounds and Carbonaceous Particles

Antonius Indarto

DISSERTATION.COM



Boca Raton

Theoretical Modelling and Mechanistic Study of the Formation and Atmospheric Transformations of Polycyclic Aromatic Compounds and Carbonaceous Particles

Copyright © 2010 Antonius Indarto

All rights reserved. No part of this book may be reproduced or transmitted in any form or by any means, electronic or mechanical, including photocopying, recording, or by any information storage and retrieval system, without written permission from the publisher.

Dissertation.com
Boca Raton, Florida
USA • 2010

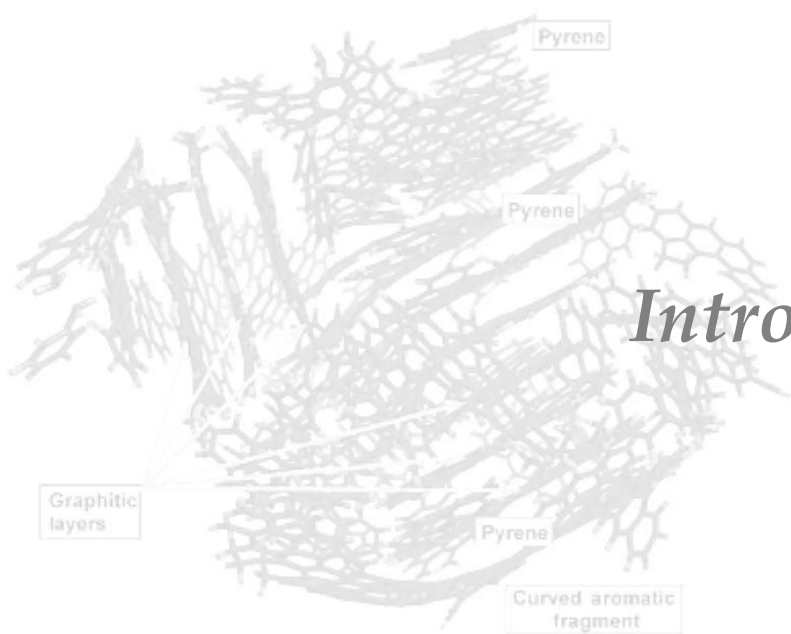
ISBN-10: 1-59942-334-0
ISBN-13: 978-1-59942-334-0

Index

Index	3
1. Introduction	5
1.1. PAH and soot characteristics	7
1.2. PAH and soot growth models	9
1.3. Purpose of the study	16
2. Computational methods	18
2.1. Density Functional Theory	19
2.1.1. Dispersion-corrected Density Functional Theory (DFT-D)	19
2.1.2. M052X functional	20
2.2. Multi-configurational self-consistent field (MCSCF)	21
2.3. Rice Ramsperger Kassel Marcus (RRKM) theory and master equation	22
2.4. Computational strategy	25
2.4.1. Part A: van der Waals interactions and PAH growth mechanism in the presence of a carbonaceous particle	25
2.4.2. Part B: Radical breeding polyene-based mechanism	27
2.4.3. Part C: First ring formation by propargyl radical and butadiyne reaction	29
3. Van der Waals interactions	31
3.1. Benzene-ethyne complex	33
3.2. Benzene-ethene complex	41
3.3. Benzene-vinyl radical complex	48
4. PAH growth in the presence of carbonaceous particulate	53
4.1. The adsorption modes	55
4.1.1. Dimer complexes	56
4.1.2. The phenyl radical adsorbed onto ovalene	57
4.2. Chain elongation in the gas and adsorbed phase	59
4.2.1. Chain elongation pathways in gas phase	60
4.2.2. Chain elongation pathways in adsorbed phase	64
4.3. Competition between chain elongation and ring formation	67
4.3.1. Gas phase pathways	68
4.3.2. Adsorbed phase pathways	72

4.3.2.1. Cyclization	72
4.3.2.2. Chain elongation	73
4.3.2.3. H loss and H abstraction	75
4.3.2.4. 'Perpendicular' adsorption	76
4.4. Effects of the carbonaceous surface shape, area, and electronic structure	79
5. Radical breeding polyyne-based mechanism	84
5.1. Model 1 ($C_4H_2 + \cdot C_4H_3$)	86
5.2. Model 2 ($C_6H_3 \rightarrow c-C_6H_3$)	88
5.3. Model 3 ($C_{10}H_5$)	90
5.4. Model 4 ($\cdot C_3H_3 + C_4H_2$)	93
5.5. Model 5: cycloaddition of two polyyne molecules	96
6. First ring formation by propargyl radical and butadiyne reaction	99
6.1. <i>Ab-initio</i> potential energy analysis	102
6.1.1. Entrance reactions	104
6.1.2. Ring transformation reactions	107
6.1.3. H migration	108
6.2. Kinetic of RRKM and master equation	108
6.2.1. Kinetic parameters	109
6.2.2. Results and discussion	110
7. Conclusions	114
Acknowledgements	118
References	119

Chapter 1



Introduction

Combustion is a primary process emitting hazardous air pollutants, *e.g.*, CO, CO₂, nitrogen oxides (NO_x), sulfur oxides (SO_x), formaldehyde, acetaldehyde, benzene, polycyclic aromatic hydrocarbons (PAHs), and soot. At first, the formed solid particles were thought of as a useful by-product of combustion which could be treated as black carbon-like material. Only as of the early 1970s, people began to find that its negative impacts are more than its positive ones, both for human health and environment. Later on, soot formation was studied worldwide. Small soot particles can be breathed deeply into the lungs where they can do substantial damage. Combustion related particulate matter is associated with a host of severe impacts such as heart attacks, stroke, cardiovascular death¹ and lung cancer² in adults. For the children, fine particles are associated with upper and lower respiratory impact, as well as retardation of lung growth.³ Soot particles from Diesel engines adsorb onto their surface some metals and toxic substances, such as cancer-causing aldehydes and PAHs. Greater concerns are arising as the presence of PAHs was detected in many urban areas.⁴ Therefore, a great attention was drawn to the chemistry of soot, PAH and hydrocarbons like 1,3-butadiene, benzene, and toluene by the scientists all over the world. Thus, the chemistry of rich flames, particularly that involved with hydrocarbon growth into PAH and soot, became one of the most active research areas in combustion chemistry. It has been known that soot comes from many different sources which result from incomplete combustion or pyrolysis.

During incomplete combustion, coal and oil components decompose into various fragment molecules, *e.g.* ethyne, small aliphatic hydrocarbons, hydrogen, radicals, *etc.* These fragments will re-react and possibly produce larger molecules, such as PAHs and soot. This fact will give a clear message for us to study well about the soot, how it comes, the details of the formation mechanism, the related kinetics is, and finally how to reduce its production.

1.1. PAH and soot characteristics

Soot is not a solely product of incomplete combustion and is usually accompanied by the presence of PAHs,⁵ nanosized carbon particles, some fullerenes,⁶ and other chemicals. The chemical structure of soot is similar to that of PAHs on the atomic level, *i.e.* a honeycomb-like network of sp^2 carbons. Captured under an electron microscope, soot appears as necklace-like agglomerates composed of a selection of small, basic particles with nearly spherical structure.

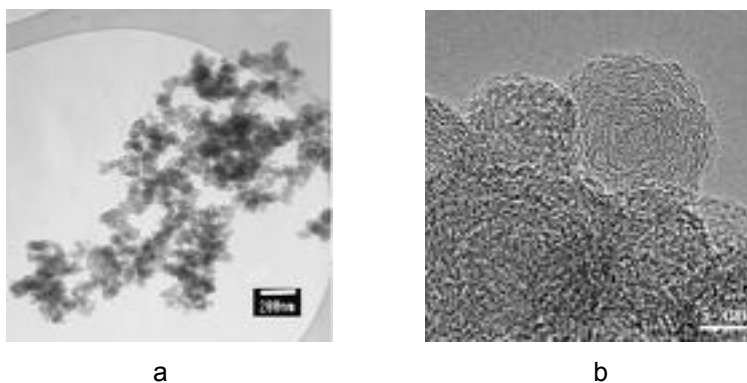


Figure 1.1. Transmission electron microscope (TEM) images of soot contains:
(a) necklace-like agglomerates and (b) numerous concentric crystallites

Individual Diesel soot particulates vary in shape from clusters of spherules to chains of spherules, where a soot cluster may contain as many as 4000 spherules. The size of spherules varies in diameter from 10 to 80 nm, but mostly lies between 15 and 30 nm. The spherules are called primary soot particles and the cluster- or chain-like soot aggregates are defined as secondary particles, composed of tens to hundreds of primary spherical particles.⁷ The transmission electron microscopy studies show that the primary soot particles have a layered structure and consist of numerous concentric crystallites.⁸ The X-ray diffraction analysis indicates that the carbon atoms of a primary soot particle are packed into hexagonal face-centered arrays commonly described as platelets. These platelets are arranged in layers to form crystallites, and there are typically

2-5 platelets per crystallite. The mean layer spacing is 3.55 nm, only slightly larger than that of graphite.⁹ The thickness of crystallites is about 1.2 nm, and they are of the order of 10^3 crystallites per primary soot particle.

The crystallites are arranged in a layered structure, parallel to the particle surface. Dislocation by five- and seven-membered rings produce surface wrinkling or layer disorder. This arrangement corresponds to the presence of turbostratic layers.¹⁰ The layered structure of soot particles is also characteristic of pyrolytic graphite, which is thought to be responsible for its unusually high resistance to oxidation. If analyzed under high-resolution transmission electron microscopy, two distinct parts of a primary Diesel soot particle can be identified; an outer shell and an inner core,¹¹ shown by schematic soot model in Figure 1.2.

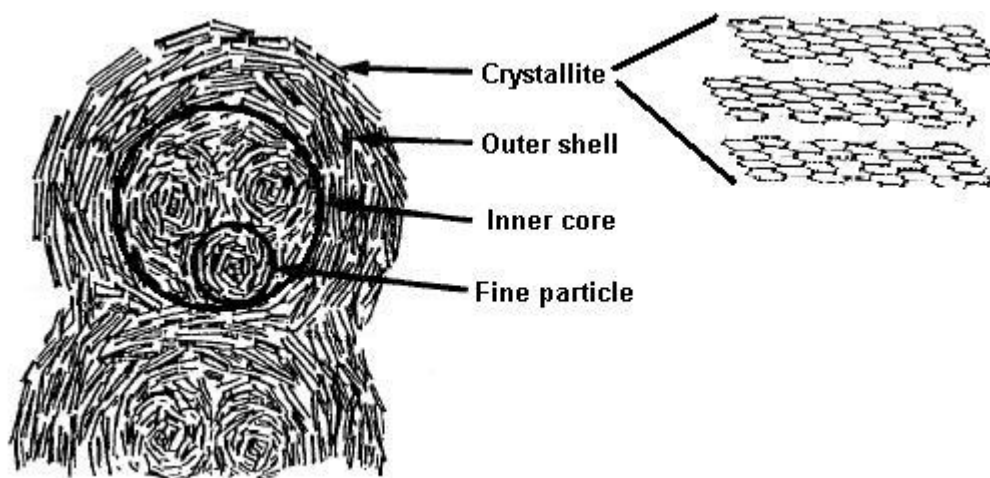


Figure 1.2. A microstructure interpretation model of the Diesel soot particle.¹¹

The platelet model mentioned above applies to the outer shell which is composed of graphitic crystallites (rigid structure). However, the inner core contains fine particles with a spherical nucleus surrounded by carbon layers with a distorted structure (low-crystallized structure). These layers are not well arranged and less dense than the outer shell. As a result, this turbostratic structure will be thermodynamically less stable and easier to be oxidized by chemical reaction.

Computational study about the structure of soot clearly mentioned the

presence of this layer formation.¹² However, this phenomenon will not be similar for every situation and can be affected by many factors. Heat treatment, for example, can alter the internal microstructure of the particles. Moreover, the particles produced in situ are also quite different from those formed in exhaust gases.

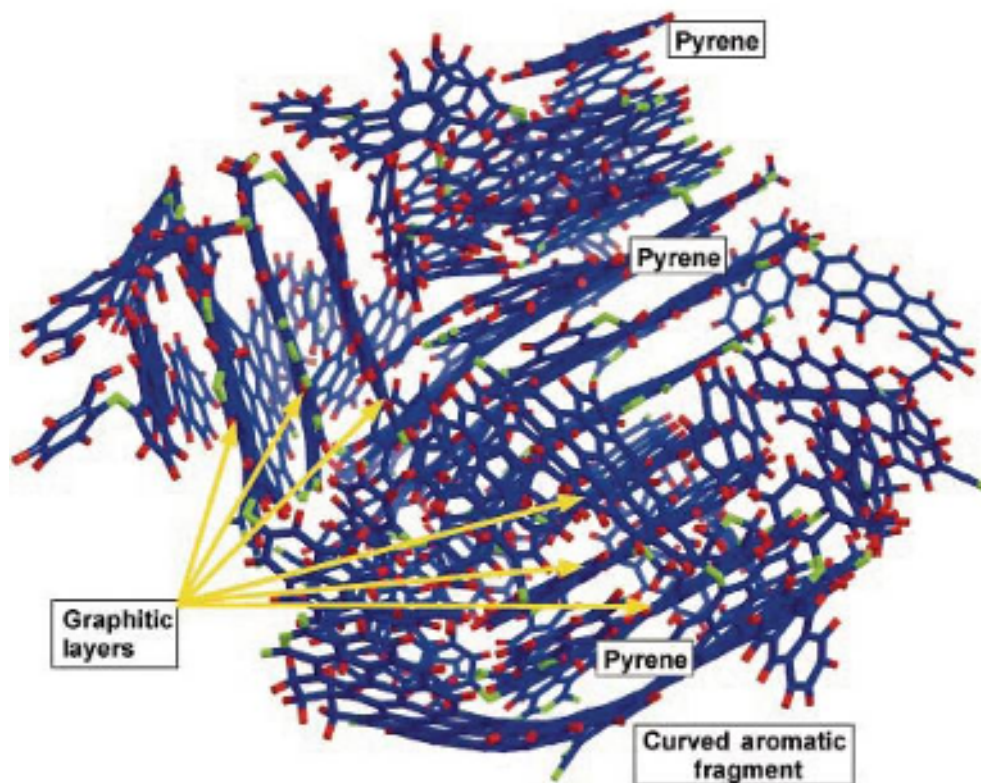


Figure 1.3. Computational image of soot simulation¹²

1.2. PAH and soot growth models

The formation of PAHs and soot is not well understood due to limited identification and quantitative measurement of the numerous intermediates and product species in combustion. Currently, some mechanisms have been proposed aimed to describe the general nature of soot particle inception; these are based on polyacetylenes, ionic species, or polycyclic aromatic hydrocarbons (PAH), considered as the key precursors to soot. The most accepted hypothesis is the

soot formation through the PAH-based growth model.¹³ Following the PAH hypothesis, a growing mechanism of soot formation should consist of several stages. Under pyrolysis or oxidation conditions, starting from the fragmentation of fuel molecules, *e.g.* an aliphatic fuel, first smaller hydrocarbon molecules and free radicals are produced. Benzene (and/or phenyl) is believed to be a basic unit in the combustion synthesis of PAHs and soot.^{14,15} This first ring seems to be the nucleus for the formation and growth of PAH, following different mechanisms.^{9,16-19} At the initial stage, the first ring is built from small aliphatic radical and molecules via radical molecule addition pathways.

Currently, using relatively advanced analysis tools, *e.g.* synchrotron vacuum ultraviolet, some small aliphatic radical and intermediates can be identified. Propargyl radical ($\cdot\text{C}_3\text{H}_3$) and butadiyne (C_4H_2) were identified in a premixed laminar flame, as shown in Table 1.1, in higher fraction compared to other small radicals or molecules.²⁰⁻²² This suggests that these two species could be the main building block in combustion processes, and hold an important role for within the mechanism of growing PAH.

Table 1.1. The concentration of propargyl radical ($\cdot\text{C}_3\text{H}_3$) and butadiyne (C_4H_2) in flames, expressed as maximum molar fraction.

Flame type	$\cdot\text{C}_3\text{H}_3$	C_4H_2
benzene/oxygen/argon ^a	2.4×10^{-3}	6.3×10^{-3}
ethyne/oxygen/argon ^b	2.1×10^{-3}	4.4×10^{-3}
lean acetone/oxygen/argon ^c	5.1×10^{-6}	-
lean n-propanol/oxygen/argon ^c	4.3×10^{-5}	-
lean i-propanol/oxygen/argon ^c	4.8×10^{-5}	-
rich acetone/oxygen/argon ^c	3.5×10^{-4}	3.2×10^{-4}
rich n-propanol/oxygen/argon ^c	3.3×10^{-4}	4.7×10^{-4}
rich i-propanol/oxygen/argon ^c	3.4×10^{-4}	2.4×10^{-4}

Note: ^aSee reference 20; ^bSee reference 21; ^cSee reference 22.

Once the ring molecule is formed, addition of small molecules, *e.g.* ethyne, ethene, butadiyne, *etc.*, will enlarge the size of the molecule. As regards the further growth of aromatic hydrocarbons (after the first ring molecule is

formed), the HACA (H-abstraction C_2H_2 -addition) mechanistic model is the most widely accepted one. In this mechanism, the addition of ethyne to an aromatic radical, like phenyl, leads to the new aromatic ring formation. Depending on the neighboring ring structure, the newly formed ring can either be radical, which can grow readily by adding ethyne, or it may be a closed shell molecular species. The continuous addition of ethyne was originally proposed by Bittner and Howard.²³ Moreover, the second mechanism, which is originated from Frenklach's idea,²⁴ will have to be activated through the H-abstraction reaction to produce a PAH radical species, before it can undergo the further growth reaction with ethyne. As this mechanism relies much on the presence of ethyne, the reaction rate of PAH growth seems to depend solely on the concentration of ethyne. This is a reasonable idea; however, a combustion process is a complex reaction in which many factors can influence both the reaction mechanism and reaction rate.

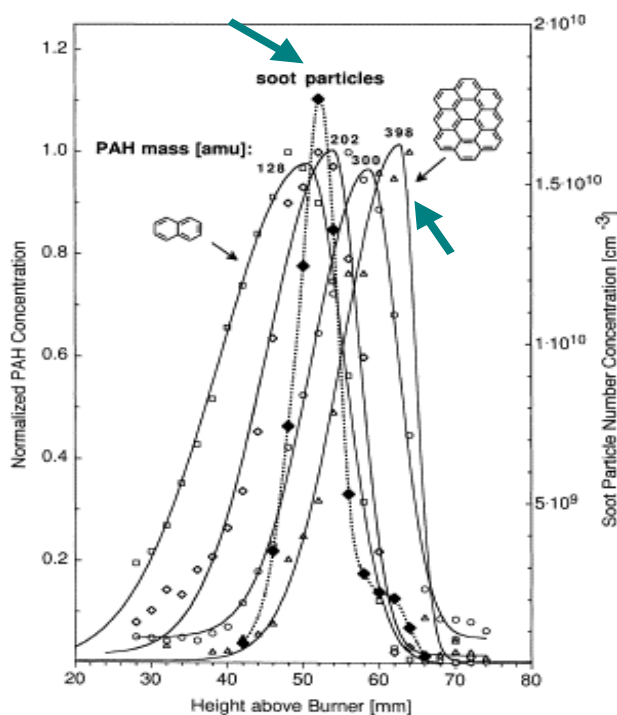
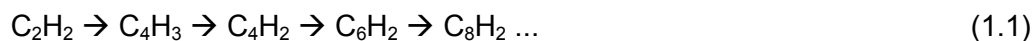


Figure 1.4. Normalized PAH concentration and particle number concentration as a function of height above burner.²⁵ Note: the two arrows show the presence of soot earlier than large PAH molecules.

One of the most interesting investigations of PAH growth in flame came from Siegmann's group.²⁵ The authors found in their 2002 experiments that the larger PAHs were formed later than soot particles. This result seems to oppose the previous idea that PAHs act as soot precursors, following the experimental observation that the concentration of PAHs decreased in order to form soot. In conclusion, the authors proposed that the particles (soot) are the precursors for PAHs, by a PAH growth mechanism favored by their adsorption on the surface of the particles. The experimental finding illustrated in Figure 1.4 also opens the possibility of another mechanism of soot formation.

Instead of ethyne, other species, such as polyynes, have been considered as the starting reagent for the PAHs and soot growth mechanism, such as polyynes. This idea was initiated by Homann and Wagner²⁶ who found that a group of species disappeared rapidly during soot growth and were no longer detected at the end of the oxidation reaction zone. The presence of butadiyne, C_4H_2 , have been measured mass-spectrometrically by Bradley & Kistiakowsky²⁷ and Gay *et al.*²⁸ as products of C_2H_2 oxidation and found that their concentration dropped sharply at the end of flame zone. Gay, *et al.*²⁸ and other authors²⁹ mentioned a step-wise chain reaction with butadiyne as the active intermediate and concluded that the reaction proceeds as:



Later on, the above mechanism was kinetically checked by an isotopic bi-mixture of ethyne ($C_2H_2 + C_2D_2$) experiment and the result was consistent with the proposed mechanism. In another experiment Bohne and Wagner observed that higher polyacetylenes are formed in premixed flat flames of C_2H_2 , C_2H_4 , C_3H_8 , C_6H_6 , and C_2H_5OH in fuel-rich mixtures, where such molecules up to $C_{12}H_2$ have been detected experimentally. Homann and Wagner²⁶ investigated the hydrocarbons occurring in the region of carbon nucleation in ethyne and benzene/oxygen flames and discussed the role of polyacetylenes and polycyclic aromatics in the process of particle inception. These authors suggested that the soot precursors can be derived by the following scheme:



A more detail explanation on the role of polyynes and PAH was put forward by Crittenden and Long.³⁰ Since they found the presence of polyynes, they proposed a mechanism (shown in Figure 1.5), apt to separate cyclization (which leads to PAH growth) and dehydrogenation reaction (leads to the formation of polyynes). At first, polymerization of ethyne produced longer-chain molecules ($C_{x>5}H_y$). From this point, the reaction went continuously into two different pathways, dehydrogenation reactions to form polyacetylene and cyclization reactions. The above ideas are similar to the conclusion, to which came Ishiguro *et al.*¹¹, that PAH growth and chain-like structure formation would occur simultaneously. A further important step was done by Kern *et al.*^{31,32} who successfully measured the product profiles during pyrolysis of ethyne, butadiene, benzene and toluene. These authors found that the main products of the reactants decomposition were polyynes: C_4H_2 , C_6H_2 , C_8H_2 .

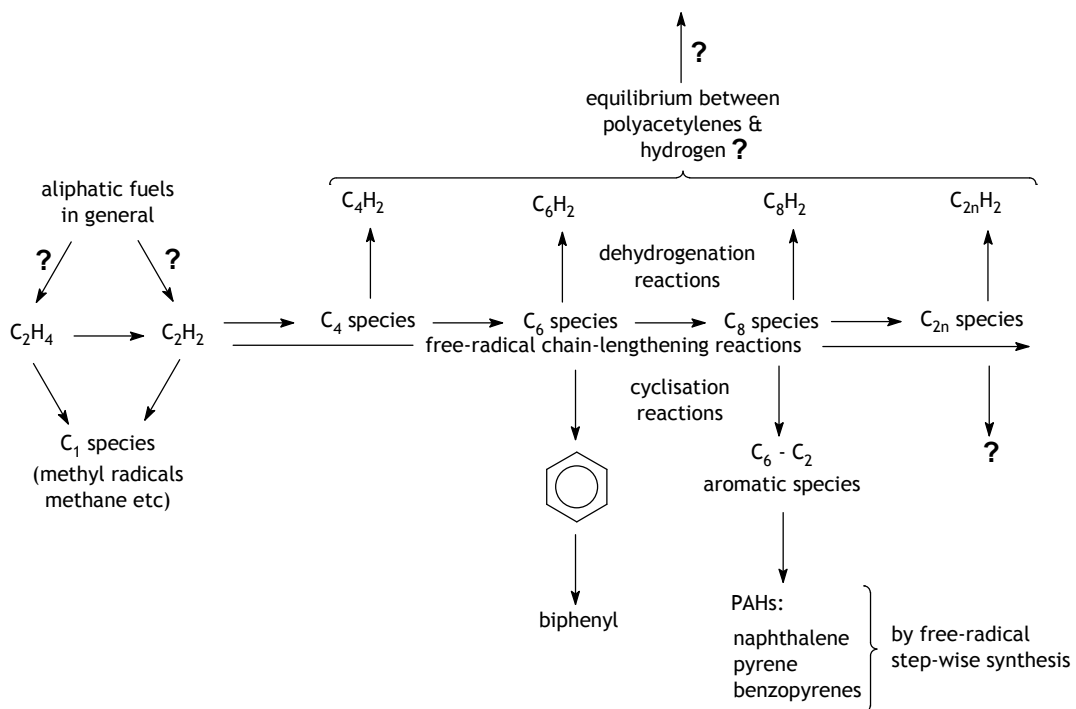
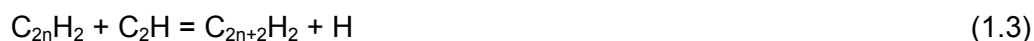


Figure 1.5. Reaction scheme suggested to account for the formation of polyacetylenes and PAH in rich premixed flames.³⁰

Nevertheless, the polyacetylene hypothesis, describing the soot inception by means of the formation of long and stable polyacetylene chains, has not been elaborated further until the work of Krestinin.³³ The author developed a detailed kinetic model of soot formation called polyynes model due to high reactivity of these species in polymerization reactions. The polyynes model is applied within soot formation simulations during pyrolysis of C_2H_2 .³⁴ A modified and extended version was further applied for soot formation modeling during pyrolysis of different hydrocarbons in reactive flow experiments.^{35,36} The model treats soot formation as a process of chemical condensation (polymerization) of supersaturated polyynes vapor ($C_{2n}H_2$) and describes the formation of young soot particles and mature soot particles, and the transformation between them. In the model, the soot formation follows three phases which take place stepwise.

(1) The growth of polyynes, follows the reactions



The above reaction is the basis of the polyynes model taken from the calculation of Kiefer and Von Drahsek³⁷ regarding the kinetic of soot formation from radical in gaseous phase. Compared to the PAH model, the polyynes grow in a simple and fast way. These reactions occur until polyynes reach their maximum stable length. In the flame, the highest polyynes detected by measurements are $C_{16}H_2$.

(2) Later, as a very long polyynes is less stable, two or more polyynes will collide forming a more stable compound and start to form new radical sites due to cyclization process. However, this mechanism is still not clear on how the molecule forms a cyclic-molecule, since polyynes has a straight chain structure. More detailed explanation of soot nuclei was described³⁸ and proposed to follow the similar pattern of the reactions:

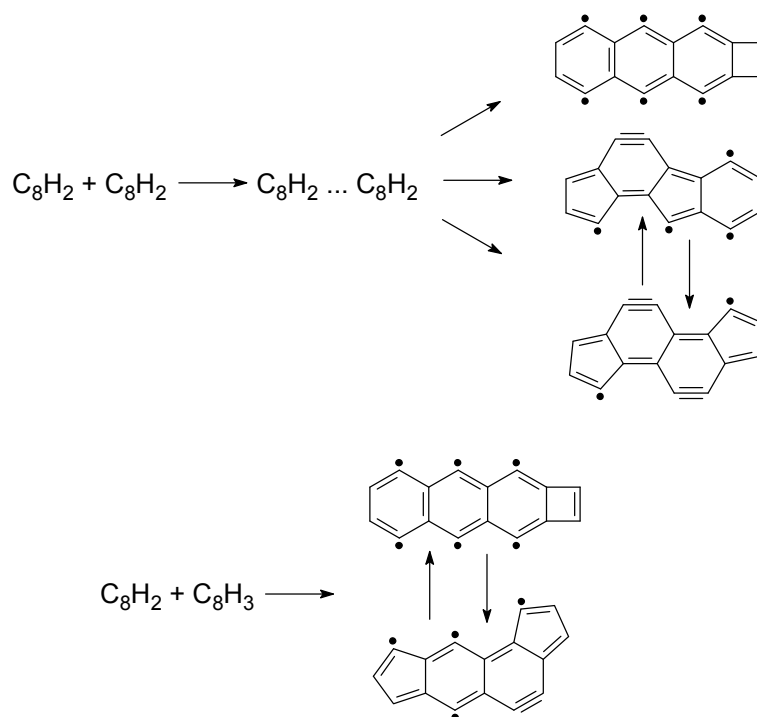


Figure 1.6. The possible pathway of soot nucleation.³⁸

The adduct molecule is very reactive as it contains more than one radical site. This type of molecule could be the nuclei of the soot growth.

(3) The termination process will occur when the number of radical is reduced, as could be made possible by collision with other radicals to form larger molecule. Until this stage, the soot fraction has reached ~40-50% of its final volume.

A more detailed soot model has been implemented to predict soot formation behind shock waves and describes the soot nucleation as a combination process of the fast polymerization of supersaturated polyene and the PAH coagulation.³⁹ Four gas phase mechanisms have been included in that model, *i.e.*: a complete set of the PAH formation reactions, the reaction mechanisms of ethyne pyrolysis, the formation of polyene molecules, and the formation of small pure carbon clusters. It was concluded that polyene molecules (*i.e.* $C_{2n}H_2$, $n=2-6$) provided a major contribution into the surface growth of soot particle. The sole HACA model for soot formation would be too slow to explain the real yield of soot. More recently, Wen *et al.*⁴⁰ developed the formation of soot

precursors model from both the detailed PAH nucleation mechanism and polyynes pathways. The model, so-called aerosol dynamics soot model, includes the comprehensive physical process, e.g. phase transition, thermal restructure, agglomeration, etc., into the detailed chemistry. The presence of polyynes improved the prediction due to short induction reaction time and fast mass growth rate of soot formation.⁴⁰

1.3. Purpose of the study

In general, this study would like to address the issue of PAHs and soot growth through the use of computational models. In accordance to the above discussion, the investigation was divided into three parts.

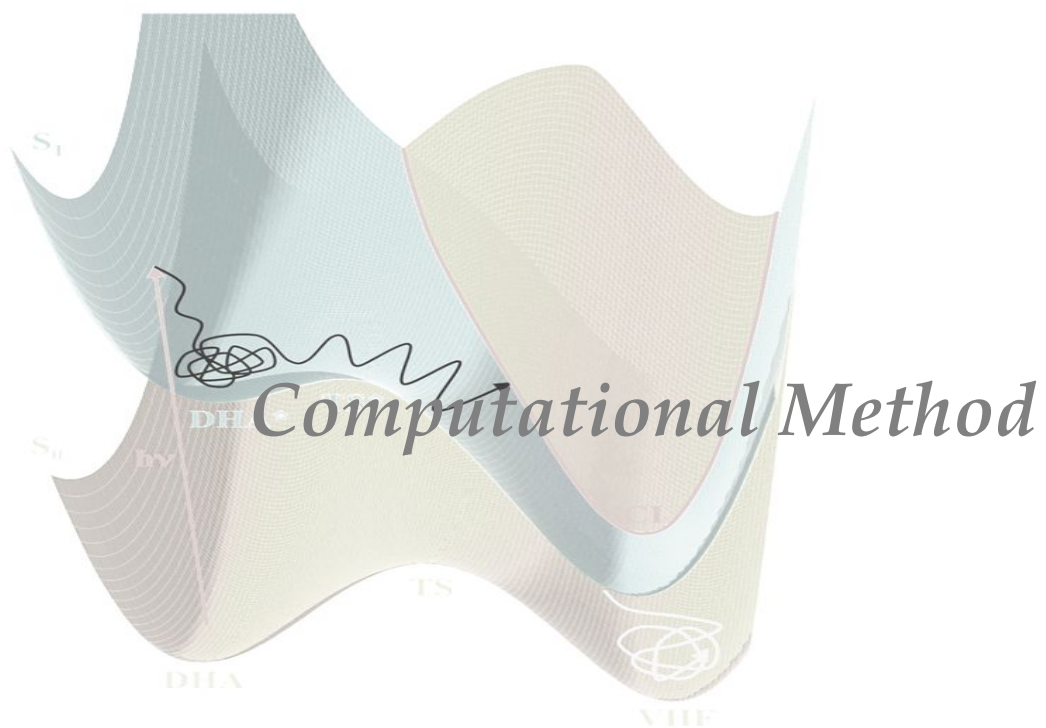
The first part deals with a model of PAH growth following the Bittner and Howard¹⁴ mechanism in the gas phase and in the presence of carbonaceous particulate. As regards this point, we would like to specifically address the experimental results of Siegmann's group, who mentioned the significant role of particulate in the formation of PAHs.²⁵ By analyzing the thermochemistry results, we could assess whether the carbonaceous particulate really has a significant role in the formation of PAH. Prior to studying the reaction model, we also devoted a study to adequately model the presence of dispersion forces (van der Waals interaction) in the growing adsorbed system. Some interaction models of limited-size, apt to investigate the problem by a variety of theoretical methods, were used. The complete description of this matter will be presented in the next section.

In the second part, we would like to address the possibility of radical breeding within a polyynes mechanism based on Krestinin's idea.^{33-36,38} The polyynes model seems to have an important role in the combustion processes in agreement with kinetic simulation.⁴⁰ However, the kinetic simulation has a weakness as the reaction rate constant (k) of soot nuclei formation from polyynes was obtained based on the estimation values, not real experimental observation. In this part, the radical breeding models were simulated by current high computational level method (multiconfiguration methods) in order to obtain reliable information. At the end, the extent to which the radical breeding mechanism may

influence the PAH and soot growth mechanism is assessed.

The very initial stage of PAHs and soot formation reactions will be addressed in the last part. The formation of first aromatic ring was suggested to be a crucial step of the PAHs and soot growth mechanism.^{14,15} In general, four-, five-, six-, or seven-membered ring molecules could be formed by the addition reaction of two hydrocarbon molecules. To examine this particular aspect, we chose the propargyl radical (C_3H_3) and butadiyne (C_4H_2) as the initial reactants, since they are found at relatively high concentrations in flame experiments.²⁰⁻²² Following an initial addition, their adduct intermediate can form a ring molecule and undergo subsequent rearrangement. All possible molecular structures were considered and the viability of each channel was assessed through a “RRKM + master equation” kinetic study.

Chapter 2



This chapter will describe briefly the computational methods used in this research, as well as their reach and their limitations, to highlight the choices made for the methods employed in this research. The computational strategy to deal with each particular case will be discussed in the last section of this chapter.

2.1. Density Functional Theory

Density functional theory (DFT)^{41,42} theory is among the most popular and versatile methods available in condensed-matter physics, computational physics, and computational chemistry. The main idea of DFT is to describe an interacting system via its electron density and not by a many-body wave function. Hence the name density functional theory comes from the use of functionals of the electron density. Compared to *ab initio* methods, such as post-SCF methods based on a Hartree-Fock⁴³ calculation (as Møller-Plesset perturbation theory⁴⁴, configuration interaction, or coupled cluster⁴⁵), the computational costs of the DFT method are relatively low and quite satisfactory for large computational model. In this investigation, the DFT methods were employed for most investigations of the PAHs growth models, especially in the first part of the study where large molecular structures were used as computational models.

2.1.1. Dispersion-corrected Density Functional Theory (DFT-D)

A drawback of most DFT functionals is that there are still difficulties to properly describe small intermolecular interactions, such as van der Waals forces (dispersion).⁴⁶ Their poor treatment of dispersion renders DFT unsuitable for the treatment of systems which are dominated by this effect (*e.g.* interaction of stacked benzene dimer) or where dispersion contributes significantly together with other effects (*e.g.* in biomolecules). Taking as an example Becke's three-parameters functional combined with Lee, Yang, and Parr's correlation functional (B3LYP),^{47,48} which is one of the most popular DFT functionals in current

computational chemistry, it was found to fail in evaluating the attractive dispersion interaction between hydrocarbon molecules.^{49,50} The development of new DFT methods designed to overcome this problem, by alterations to the functional or by the inclusion of additive terms, is a currently hot research topic.

Dispersion is an intermolecular electron correlation effect and some relatively high level computational methods, like second-order Møller–Plesset perturbation theory (MP2),⁴⁴ describe dispersion relatively well. However, MP2 calculations are far more expensive than DFT calculations. Currently, in the scheme of the DFT approach, there are two common ways to describe correctly the presence of dispersion in the functionals. A pragmatic solution is adding a ‘damped dispersion’ term calculated from parametrised atom–atom contributions to standard functionals like PBE or B3LYP⁵¹⁻⁵⁵ and the total potential energy (E_{total}) will be the contribution from both ‘pure’ DFT and dispersion energy.

$$E_{total} = E_{DFT} + E_{disp} \quad (2.1)$$

while E_{disp} is an empirical dispersion correction given by

$$E_{disp} = -s_6 \sum_i \sum_j \left(\frac{C_6^{ij}}{R_{ij}^6} \right) \left(\frac{1}{(1 + \exp(-\alpha(R_{ij} / R_0 - 1)))} \right) \quad (2.2)$$

where R_0 is the sum of atomic van der Waals radii and α is a parameter determining the steepness of the damping function. The value of the atomic C_6 coefficients, and the R_0 , α , and s_6 parameters were obtained following the work of Grimme.⁵²

Since the dispersion interaction, a type of attractive interaction between two substrates, is important in the adsorption process of PAHs on soot, *i.e.* carbonaceous particulates, the use of DFT-D functional could be advisable.

2.1.2. M052X functional

As mentioned above, instead of adding a damped coefficient term to the standard functional, another solution to improve DFT performances is implemented by re-parametrising the different exchange and correlation terms with some mixture of Hartree-Fock (hybrid) functionals. This is based on the fact

that the accuracy of a DFT calculation depends upon the quality of the exchange-correlation (XC) functional. For this purpose, the Truhlar group, for example, has designed a newly class of functional, called M05-class⁵⁶ to obtain a better prediction of the thermochemistry-kinetics problems and noncovalents interactions. The exchange-correlation M05 class functional, like M05-2X, was built by optimizing the parameters of correlation and exchange functionals with inclusion of kinetic energy density (hybrid meta) in the functional. Some percentages of Hartree–Fock contribution have been included in the total exchange energy. At the end, the final XC functional will be of the form:

$$E_{XC}^{hyb} = \frac{x}{100} E_X^{HF} + \left(1 - \frac{x}{100}\right) E_X^{DFT} + E_C^{DFT} \quad (2.3)$$

where E_X^{HF} is the Hartree–Fock exchange energy, E_X^{DFT} is the DFT exchange energy, and E_C^{DFT} is the DFT correlation energy. X, the percentage of Hartree–Fock exchange in the hybrid functional, is equal to 56, much higher than in B3LYP ($X_{B3LYP} = 20$).⁵⁶

Zhao *et al.*⁵⁶ mentioned that the M05-2X functional gives optimum results for a combination of nonmetallic thermochemical kinetics, thermochemistry, and noncovalent interactions. The M05-2X method also gives the best performance for the calculation of absolute and relative bond dissociation energies for single-reference systems and for calculations of noncovalent interactions between molecules.^{56,57} This approach introduces of course some kind of semiempirical character in the DFT scheme.

2.2. Multi-configurational self-consistent field (MCSCF)

In some cases, when the reaction deals with complex chemical situations, e.g. the presence of di- or multi-radical sites in a molecule, methods as density functional theory, which is usually set as an intrinsically single-reference method, is not adequate to assess safely the electronic and energetic traits. The diradical nature of a species, for instance, implies an intrinsically multiconfigurational trait of its wavefunction. Multi-configurational self-consistent field (MCSCF)⁵⁸⁻⁶⁰ is a solution to generate qualitatively correct reference states of this kind of molecules.

It uses a linear combination of configuration state functions (CSF), or determinants, to approximate the exact electronic wavefunction of an atom or molecule. This kind of method is useful in particular to study, within this Thesis work, the radical breeding mechanism of polyyne model, since multi radical sites can be present in a single molecule.

The MCSCF calculations require the definition of an active space of m orbitals, in which every possible arrangement of the n 'active' electrons are taken into account (complete active space, CAS). In this space a full CI is performed, and the orbitals are optimized as well. MOs are included which are more directly involved in the bond breaking/bond making processes (the chosen active space is defined in general with the aid of the graphical, 3-dimensional, analysis of the orbitals generated by some preliminary lower-level calculation). The detailed active space used for the radical breeding model will be presented in the next section. The CAS(n,m)-MCSCF calculation (CASSCF for short) takes into account most of the non-dynamical structure dependent correlation energy.

To get a better assessment of each critical point energy, a multi-reference second-order perturbation (CASPT2) calculation is then carried out, which takes into account a good share of the dynamical correlation energy.⁶¹⁻⁶³ Unfortunately, CASPT2 is a computational demanding method, which requires large resources and rather long calculation times. Then, in general, the geometries are not re-optimized at this level (which could be done by numerical gradient methods), but a single point calculation over the optimized CASSCF geometry is performed.

2.3. Rice Ramsperger Kassel Marcus (RRKM) theory and master equation

The Rice Ramsperger Kassel Marcus (RRKM) theory⁶⁴ is widely used to interpret the behavior of thermal and photochemical reactions.⁶⁵ RRKM is one of the fundamental development of unimolecular kinetic based of the Lindemann mechanism⁶⁶ and its development by Hinshelwood⁶⁷. Treatment of molecular vibrations and rotations are the key point in this theory.

When a molecule reacts via a unimolecular reaction to form an intermediate, this intermediate could have an excess of rovibrational energy E^* .

By collisions with buffer gas, part of E^* is dispersed and after an adequate number of collisions, a thermal energy distribution (Boltzmann's distribution, thermal equilibrium) is reached. At transition state, the excess of energy becomes $E^+ = E^* - E_0$, where E_0 is the energy barrier. Conventionally, all the energies include the zero point corrections.

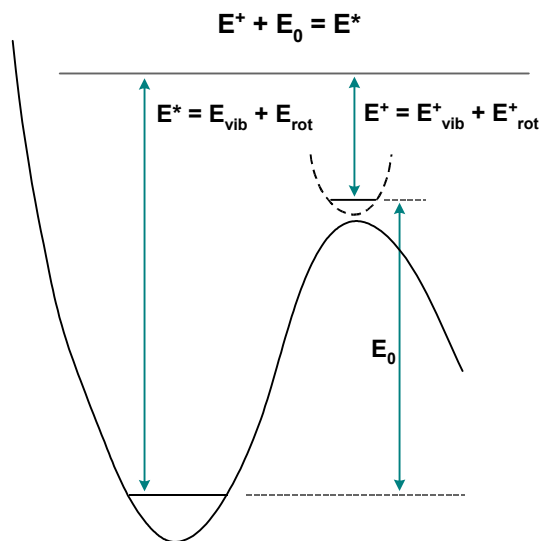


Figure 2.1. Illustration of potential-energy surface for unimolecular reaction.

The rate constant to overcome the E_0 barrier is function of the energy E^* of the system: at high energy reaction is fast, and when E^* is below E_0 , rate constant is zero by definition. RRKM theory describes the changes of the rate constant with the energy. It is possible to demonstrate that:⁶⁴

$$k(E^*) = \frac{W(E^+)}{h \rho(E^*)} = \frac{1}{h} \frac{W(E^* - E_0)}{\rho(E^*)} \quad (2.4)$$

where $k(E^*)$ is the rate constant for the unimolecular process, in s^{-1} . $W(E)$ is the sum of the states: the total number of the states between 0 and E^* . $\rho(E)$ is the density of states: the number of the states between E^* and $E^* + \delta$. The relation between $W(E)$ and $\rho(E)$ is:

$$\rho(E^*) = \frac{\partial W(E^*)}{E^*} \quad (2.5)$$

E^* or E^+ can be partitioned into vibrational (E_v) and rotational E_r energies, and $W(E)$ and $\rho(E)$ are calculated from vibrational frequencies and moments of inertia, by using exact states count algorithms.⁶⁴

$$W(E) = \sum_{E_{vr}=0}^{E_{vr}} P(E_{vr}) = \sum_{E_v=0}^{E_{vr}} P(E_v) \sum_{E_r=0}^{E_{vr}-E_v} P(E_r) \quad (2.6)$$

$$\rho(E) = \sum_{E_v=0}^{E_{vr}} P(E_v) \rho_r(E_{vr} - E_v) \quad (2.7)$$

where $P(E_v)$ is the number of vibrational states with vibrational energy of E_v and $P(E_r)$ is the number of rotational states with rotational energy of E_r .

RRKM only shows how the rate constant changes with the energy, but during the reaction the excited specie could also collide with the buffer gas. Master equation is a complex system of equations which calculates the probability of the energy loss and gain at every collision with the buffer and the probability of competition among the reactions through the rate constant $k(E)$ and energy loss and gain at every collision with the buffer gas.

$$\frac{dA_i}{dt} = \omega \left(\sum_j P_{ij} A_j \right) - \omega A_i - k_i A_i \quad (2.9)$$

where A_i is the concentration of reactant (A) in state number i (which has energy E_i), ω is the collision frequency, P_{ij} is the probability that a molecule that is in its state j before collision is in state i after a collision, and k_i is the rate constant for decomposition of A_i to give products ($k_i = k(E_i)$).

Knowing the initial E^* energy, the pressure of the buffer gas (usually N_2 , He, Ar, O_2 , etc), the type of the gas, it is possible to estimate the collision frequency (ω) between the buffer gas and the molecule and numerically solve the Master Equation. The result is the concentration of A in function of the time t (proportional to the number of collisions). At large t , collisions with buffer gas dissipate the excess of rovibrational energy and the system reaches the thermal equilibrium: in this borderline case, $k(E)$ coincides with the rate constant

calculated by transition state theory (TST):⁶⁴

$$k = \frac{1}{h} \frac{Q^\ddagger}{Q} e^{-E_0/RT} \quad (2.10)$$

where Q and Q^\ddagger are the partition functions for the intermediate and the transition structure, respectively.

2.4. Computational strategy

In general, all electronic structure calculations were performed with the Gaussian 03⁶⁸ suite of programs for DFT and CASSCF calculations, and Molcas 7.2⁶⁹ for single point CASPT2 calculations. Some other softwares (MOLPRO,⁷⁰ ORIENT⁷¹) will be used for particular purposes, and will be mentioned directly in the discussion. The Molden⁷² program was exploited for the graphics. The major parts of the optimizations were done usually without any constraints and the nature of the critical points was checked by vibrational analysis. For transition structures, which correspond to the first-order saddle points on the energy hypersurface, inspection of the normal mode related to the imaginary frequency was generally sufficient to connect them to the related energy minima. The geometry, energy, and harmonic vibrational frequencies of each stationary point considered were determined at different computational levels, as detailed for the particular cases discussed below.

2.4.1. Part A: van der Waals interactions and PAH growth mechanism in the presence of a carbonaceous particle

Although some studies have been done by using a recently proposed dispersion-corrected density functional theory (DFT-D) for some hydrocarbon systems,⁵¹⁻⁵⁵ it is still worthwhile to explore and validate the DFT-D functional as regards its capability to represent the van der Waals interaction in some models related to PAHs and soot growth, *i.e.* benzene-ethyne ($C_6H_6-C_2H_2$), benzene-vinyl radical ($C_6H_6-C_2H_3$), benzene-ethene ($C_6H_6-C_2H_4$). Recalling that soot consists also of parts constituted by of numerous condensed six-membered unsaturated carbon rings,¹¹ benzene could represent locally a single hexagonal ring. Then, its